# Turbulent Flow and Heat Transfer Characteristics of a Two-Dimensional Oblique Plate Impinging Jet

**Soon Hyun Yoon\*, Moon Kyung Kim\*\* and Dae Hee Lee\*\*\***

(Received July 18, 1996)

Turbulent flow and heat transfer characteristics of a two-dimensional oblique plate impinging jet (OPIJ) were experimentally investigated. The local heat transfer coefficients were measured using thermochromic liquid crystals. The jet mean velocity and turbulent intensity profiles were also measured along the plate. The jet Reynolds number (Re, based on the nozzle width) ranged from 10, 000 to 35, 000, the nozzle-to-plate distance $(H/B)$ from 2 to 16, and the oblique angle $(\alpha)$ from 60 to 90 degree. It has been found that the stagnation point shifted toward the minor flow region as the oblique angle decreased and the position of the stagnation point nearly coincided with that of the maximum turbulent intensity. It has also been observed that the local Nusselt numbers in the minor flow region were larger than those in the major flow region for the same distance along the plate mainly due to the higher levels in turbulent intensity caused by more active mixing of the jet flow.

**Key Words :** Oblique Plate Impinging Jet, Turbulent Flow, Heat Transfer, Liquid Crystal

## 1. Introduction

Due to the advantages of high local heat and/or mass transfer rate and a relatively easy control of areas to be cooled or heated, impinging jets are widely used in many industrial applications such as cooling of hot steel plates, annealing of glass and sheet metals, drying of papers, films and textiles, and cooling of turbine blades and electronic components, and most recently manufacturing of TFT-LCD plate.

There have been many experimental and numerical studies of the impinging jet flow and heat transfer. These studies have investigated the effects of Reynolds number, nozzle-to-plate distance, nozzle geometry, jet temperature, jet orientation, multiple jets, cross flow, and jet impinging surface curvature on the flow and heat transfer (Jambunathan et al., 1992; Viskanta, 1993)

Heat transfer measurements for various nozzle geometries and flow conditions have been made by many researchers. Gardon and co-workers (1962, 1965, 1966) investigated the local heat transfer coefficients for axisymmetric and planner, single or arrays of jets by using a thin circular foil meter. Hoogendoorn (1977) studied the effect of turbulence on the heat transfer at the stagnation point with long straight pipe and smoothly convergent nozzle. Chia et al. (1977) studied the mass transfer in axisymmetric turbulent impinging jets using the naphthalene technique. Kataoka (1990) investigated the effect of artificially-induced large scale eddies on the enhancement of impinging jet heat transfer. Baughn and his co-workers (1989, 1991, 1993) have carried out heat transfer measurements with a fully developed round jet impinging on the flat plate. More recently, Lee et al. (1994, 1995) have studied the heat transfer characteristics with an air jet issuing from an elliptical nozzle and from a long straight pipe

---

\* School of Mechanical Engineering, Research Institute of Mechanical Technology Pusan National University
\*\* Department of Mechanical Design, Chang Won Junior College
\*\*\* Department of Mechanical Engineering, Inje University

nozzle, respectively.

All of the studies referenced above have investigated the flow and heat transfer characteristics for jets impinging vertically on the flat plate. However, due to the shape of the surface or its orientation to the main jet flow, many industrial applications of the oblique plate impinging jet (OPIJ) may be encountered. The literature survey reveals that studies of heat transfer characteristics of the OPIJ are relatively rare. Sparrow and Lovell (1980) measured local mass transfer (converted to heat transfer) to the OPIJ at low Reynolds numbers less than 10, 000. They found that the point of maximum heat transfer was shifted from the geometric impingement point, with a degree of the displacement increasing with larger oblique angle, but the average heat transfer coefficient remained nearly the same. Goldstein and Franchett (1988) studied heat transfer due to the OPIJ using a temperature-sensitive liquid crystal. The jet Reynolds number studied ranged from 10, 000 to 30, 000, the jet orifice-to-plate distance from 4 to 10, and the angle between the axis of jet orifice and the plate surface from 30 to 90 degree. Their results also showed a displacement of the peak heat transfer from the geometric center of the jet origin, with the displacement being a function of impingement angle. Steven and Webb (1991) obtained a correlation between the local heat transfer coefficient and the oblique angle. Foss and Kleis (1976) investigated the mean flow characteristics, streamwise vorticity, and stagnation point location for jet oblique angles less than 12 degree. Foss (1979) measured the turbulent intensities near the impingement surface, constant pressure distribution on the surface and velocity vectors for an oblique angle of 45 degree.

The present study is aimed at investigating the flow and heat transfer characteristics of the two-dimensional turbulent jet impinging on the inclined flat plate. The jet mean velocities, turbulent intensities, and local convective heat transfer coefficients are measured by employing a hot-wire probe and thermochromic liquid crystal, respectively. The static pressure coefficients are also measured along the inclined surface. The

experiments are made for the jet Reynolds number (based on the nozzle width (B)) ranging from 10, 000 to 35, 000, the nozzle-to-plate distance $(H/B)$ from 2 to 16, and the oblique angle $(\alpha)$ from 60 to 90 degree.

## 2. Experimental Apparatus and Procedure

Measurements are made in a low speed open circuit type wind tunnel. Air is moved by 5HP centrifugal fan. The fan speed is controlled by an inverter and the corresponding jet velocity is measured with a pitot tube and electronic micromanometer to an accuracy of $\pm2\%$. The wind tunnel consists of a diffuser, plenum chamber and a contraction nozzle. The wind tunnel has a contraction ratio of 4.53 and a size of the exit nozzle is of 350 mm $\times$ 26.5 mm, resulting in an aspect ratio of about 13.2.

A schematic diagram of the experimental apparatus is shown in Fig. 1. The jet flow is classified into two regions: the major flow region in the positive S direction and the minor flow region in the negative S direction. The plate on which the
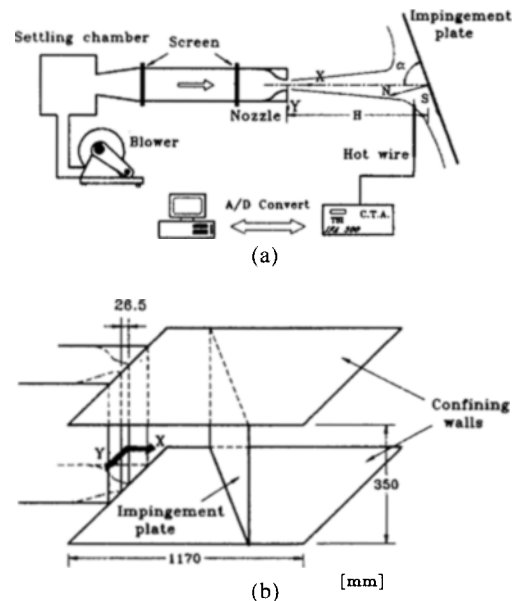


(a)

(b) [mm]

**Fig. 1** Schematic diagram of (a) the experimental apparatus and (b) test section for heat transfer measurements

discharged jet impinges was made of a 350 mm high, 1,500 mm long, and 20 mm thick Plexiglas. The impinging plate was installed such that there was an oblique angle between the jet streamwise axis and the plate surface. For the wall pressure measurements stainless steel tubes with 1 mm outer diameter were imbedded with 1 cm separation distance on the plate surface.

In order to minimize the conduction heat loss, a gypsum plate was placed above the Plexiglas plate. To the surface of the gypsum plate was glued a sheet of gold film Intrex (a very thin gold-coated polyester substrate sheet). Copper foil strip "electrodes" were then attached to either end of the surface of the Intrex and silver-loaded paint was applied to establish a good electrical contact between the copper electrodes and the Intrex surface. By passing a D. C. current through the Intrex, an essentially uniform wall heat flux boundary condition was created in the plate surface. The copper electrodes were then connected to a variable transformer in series with a current shunt (rated 50 mV and 5 amps), allowing an adjustable voltage to be supplied to the electrodes and the voltage drop across and current input to the Intrex to be measured. Two digital multimeters having a precision of 3 significant figures were used to measure the voltage across the Intrex and current shunt.

An air brush connected to a 7.5 HP compressor was used to spray first a thin layer of black backing paint and liquid crystal on the Intrex surface. The liquid crystal used in this experiment was "R35C1W" micro-encapsulated thermochromic liquid crystal. A care was taken to minimize the radiation loss for the heated surface: a fiber optic cold light source was used to illuminate the liquid crystal surface. Since the actual color image is affected by factors such as the angle and distance of the light illuminating the liquid crystal covered surface, and aging effects, a careful color calibration was carried out using a digital color image processing system.

## 3. Data Reduction

The streamwise and crosswise velocity compo-

nents in the OPIJ were measured using two constant temperature anemometers (TSI, IFA300), X and I type hot wire probes. The I type probe was calibrated using a five order polynomial equation, the X type probe using a look up table. A calibrated 0.25mm diameter Chromel-Alumel thermocouple measured the jet exit temperature to an accuracy of $\pm 0.1°C$. The measurement technique in this study, described by Lee et al. (1994, 1995) provides a method for determining the surface isotherm using liquid crystal. By electrically heating a very thin gold-coating on the Intrex, an essentially uniform wall heat flux condition is established. The heat flux can be adjusted by changing the current through the Intrex, which changes the surface temperature. Under the constant heat flux condition, an isotherm on the Intrex surface corresponds to a contour of a constant heat transfer coefficient. As the heat flux change, the position of the color isotherm also moves. The local heat transfer coefficient at the position of the particular color being observed is calculated from

$$h = \frac{q_v}{(T_w - T_J)} \qquad (1)$$

where, $T_w$ is the wall temperature determined by liquid crystal, $T_J$ is the jet temperature, $q_v$ is the net heat flux which is obtained by subtracting the radiation and conduction heat losses from the total heat flux through the Intrex; i. e.

$$q_v = \frac{f \cdot I \cdot V}{A} - \varepsilon\sigma(T_w^4 - T_a^4) - q_c \qquad (2)$$

The ratio of the local electrical heating to the average heating, f, is a measure of the uniformity of the gold coating Lee et al. (1994) found the uniformity to be as high as 98% when the test section of Intrex is small and selected from the middle of a roll where the gold-coating is most uniform. It has been the case for the present experiment. Therefore, we assume $f = 1$ for the heat flux calculation, but f is maintained in Eq. (2) because it contributes to the overall uncertainty. And in this experiment, the current shunt having a 0.05% accuracy was used for precise measurement of the current into the Intrex. The variables I, V, A, $\varepsilon$, $\sigma$, $T_a$ and $q_c$ are the current

**Table 1** Nusselt number uncertainty analysis

| $x_i$ | Unit | Value | $\delta x_i$ | $\dfrac{\delta x_i}{Nu}\dfrac{\partial Nu}{\partial x_i}\times 100\,(\%)$ |
|---|---|---|---|---|
| $f$ | | 1.0 | 0.02 | 1.97 |
| $A$ | [m²] | 0.0025 | $4.975\times 10^{-5}$ | 1.90 |
| $T_w$ | [°C] | 35.6 | 0.22 | 1.56 |
| $V$ | [V] | 11.291 | 0.125 | 1.06 |
| $I$ | [A] | 0.45 | $5.0\times 10^{-3}$ | 1.06 |
| $T_a$ | [°C] | 21.2 | 0.14 | 0.93 |
| $B$ | [m] | 0.0265 | $5.0\times 10^{-5}$ | 0.23 |
| $\varepsilon$ | | 0.9 | 0.05 | 0.21 |

Total Nu uncertainty : $\dfrac{\delta Nu}{Nu}=3.62\%$

into the Intrex, voltage across the Intrex, surface area of the Intrex, emissivity of liquid crystal and black backing paint on the surface of the plate, Stefan-Boltzmann constant, ambient temperature and conduction loss, respectively.

The uncertainty estimates using the method suggested by Kline and McKlintock (1953) show that the Nusselt number uncertainty for $H/B=6$ and $\alpha=90$ degree at Re=35, 000 is 3.62%. The uncertainty in the gold-coating uniformity factor is the largest contribution to the uncertainty. Another source of the large uncertainty is the measurement of the Intrex area.

## 4. Discussion of Results

### 4.1 Flow characteristics

Figure 2 shows the wall pressure coefficient distributions along the plate surface for the seven nozzle-to-plate distances at one oblique angle of $\alpha=90$ degree. It is shown from Fig. 2 that for all $H/B$'s, the maximum pressure coefficient occurs at the stagnation point which is also the geometric center of the plate, $S/B=0$. It is also shown that the discharged jet is mixed with the surrounding ambient air and consequently the shape of the wall pressure coefficient profiles spreads wider with increasing $H/B$.

Figure 3 shows that for all $H/B$'s tested the position of the maximum wall pressure coefficient at $\alpha=70$ degree shifted half the distance of the nozzle width to the minor flow region due to the coanda effect which is caused by the difference in
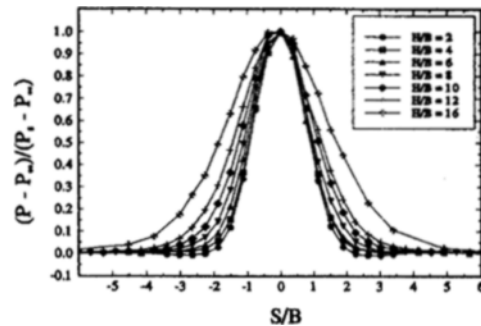


**Fig. 2** Profiles of wall pressure coefficients along the plate surface at $\alpha=90$ degree and $Re$ $=35,000$
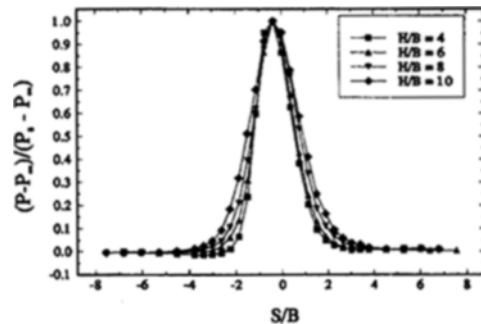


**Fig. 3** Profiles of wall pressure coefficients along the plate surface at $\alpha=70$ degree and $Re$ $=35,000$

the flow entrainment in the jet impingement region. This behavior is consistent with the results by Ichimiya (1995) who suggested that the stagnation point exists between the geometric center and the nozzle edge at $\alpha=60$ degree.
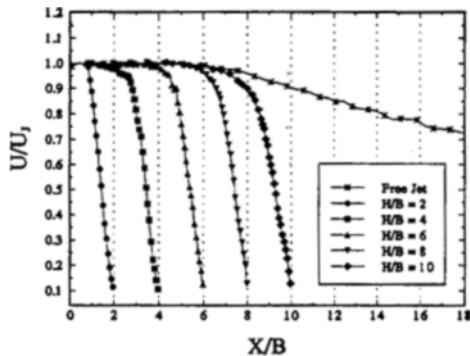
Profiles of free and impinging oblique jet

**Fig. 4** Mean velocity profiles along the free jet and impinging jet centerlines for $\alpha=90$ degree and $Re=35,000$
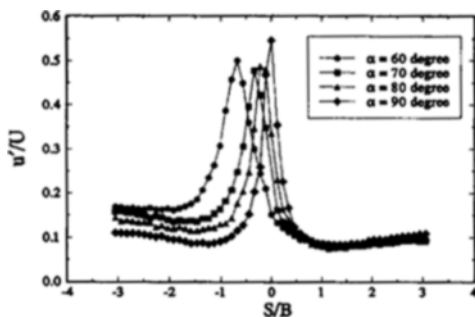


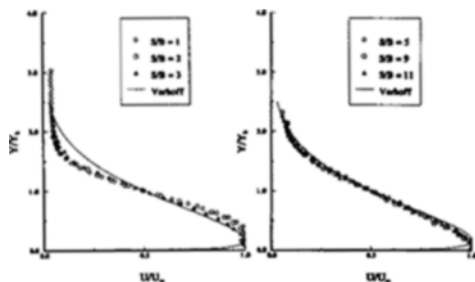**Fig. 5** Turbulent intensity profiles in the impingement region for $H/B=6$ and $Re=35,000$



**Fig. 6** Mean velocity profiles in the wall jet region for $H/B=6$, $\alpha=70$ degree and $Re=35,000$

centerline velocity for various $H/B$'s and one oblique angle of $\alpha=90$ degree are plotted in Fig. 4. From this figure, the potential core length of the free jet is estimated to be 5 nozzle widths, which is a typical value for the two-dimensional plane jet (Martin, 1977). It is also observed that the impinging jet centerline velocity profiles coincide with the free jet centerline velocity pro-

file down to the region (i. e. the beginning of the impingement region) approximately $3\sim4$ nozzle widths above the plate surface and drastically decay afterwards as the jet approaches close to the surface, which agrees well with data by Tani and Komatsu (1964).

The turbulent intensity profiles are measured at 2mm location from the plate wall are plotted in Fig. 5 for various oblique angles and $H/B=6$. Figure 5 shows that at $\alpha=90$ degree, the turbulent intensity profile is symmetric about the jet axis. It also shows that as the oblique angle decreases, the location of the maximum turbulent intensity shifts upstream progressively and its magnitude in the minor region increases. However, the oblique angle does not seem to affect much the turbulent intensity in the major flow region in which the flow is in the process of being redeveloped to the wall jet.

To investigate similarities in the flow characteristics downstream of the major flow region, the mean velocity profiles for $H/B=6$ and $\rightarrow=70$ degree are plotted against the vertical distance from the plate in Fig. 6. According to Verhoff (1963) who investigated the two-dimensional turbulent wall jet with and without an external stream, a similar behavior is observed in the present experiment for S/B $>$ 5 in Fig. 6.

**4.2   4.2 Local heat transfer characteristics**

The local Nusselt number distributions along the plate are presented in Fig. 7 for four Reynolds numbers at one oblique angle of $\alpha=60$ degree and $H/B=6$. It is observed that the Nusselt number increases with Reynolds number, with the maximum Nusselt number positions remaining the same. It should also be noted that the position of the maximum wall pressure coefficient in Fig. 3 nearly coincides with that of the maximum Nusselt number in Fig. 7.

Figure 8 represents the local Nusselt number distributions for four oblique angles and one Reynolds number of $Re=35,\ 000$ at $H/B=6$. When the jet vertically impinges on the plate, the distribution curve has a peak at the stagnation point. As the oblique angle decreases, an asymmetry in the Nusselt number distributions
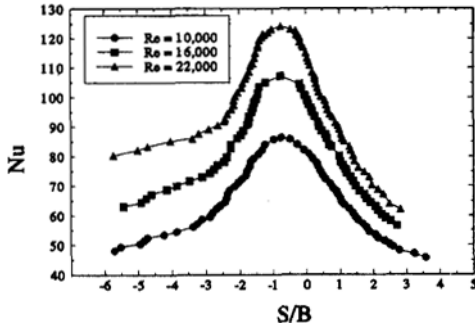
**Fig. 7**  Local Nusselt number distributions on the plate surface for various Reynolds numbers at $H/B=6$ and $\alpha=70$ degree
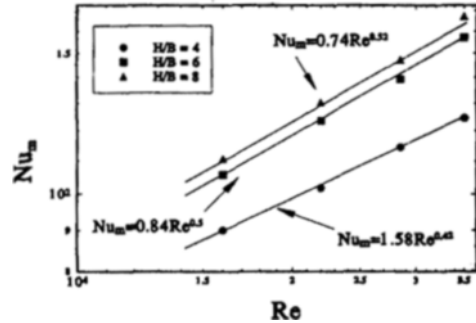


**Fig. 9**  Correlations between maximum Nusselt number and Reynolds number for various $H/B'$ s at $\alpha=70$ degree
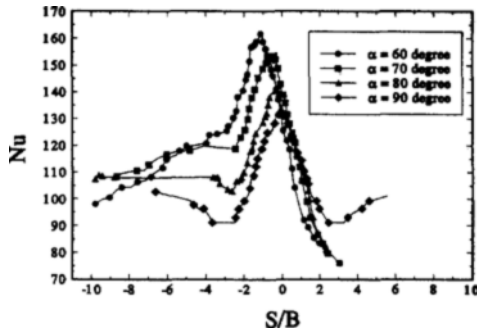


**Fig. 8**  Local Nusselt number distributions on the plate surface for various inclined angles at $H/B=6$ and $Re=35,000$
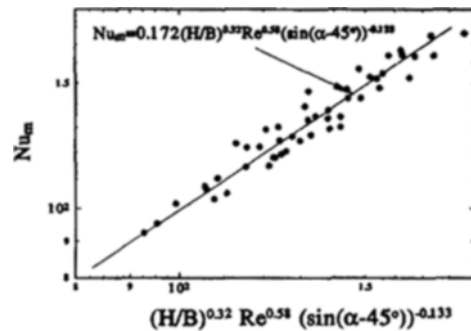


**Fig. 10**  Correlation of maximum Nusselt number in terms of $H/B$, $Re$ and $\alpha$

becomes more apparent. This phenomenon is caused by the turbulent mixing process in the minor flow region, which is presented in Fig. 5. In general, the initial momentum of the impinging jet provides a downward thrust. When the jet impinges on the inclined plate, the minor flow has to spend much of the kinetic energy to abruptly change the flow direction upward. Thus, the turbulent intensity levels near the plate in the minor flow region become stronger than in the major flow region. Consequently, the local Nusselt numbers in the minor region are higher than in the major region.

The variation of the maximum Nusselt number, $Nu_m$, with the jet Reynolds number, Re, is shown in Fig. 9 for three nozzle-to-plate distances of $H/B=4$, 6, and 8, and one oblique angle of $\alpha=70$ degree. For $H/B=4$, the maximum Nusselt numbers vary according to $Nu_m \propto Re^{0.42}$. For larger

distances, $H/B=6$ and 8, the Reynolds number dependence is stronger ($Nu_m \propto Re^{0.5}$ for $H/B=6$ and $Nu_m \propto Re^{0.52}$ for $H/B=8$).

This is attributed to an increase of turbulence in the approaching jet as a result of the stronger exchange of momentum with the surrounding ambient air, which in turn enhances the heat transfer rate. A correlation of Num in terms of $H/B$, $Re$, and $\alpha$ are plotted in Fig. 10 and obtained as follows;

$$Nu_m = 0.172 \ (H/B)^{0.32}(Re)^{0.58} \cdot$$
$$(\sin(\alpha-45))^{-0.133} \qquad (3)$$

with a scatter of 10%

## 5. Conclusions

The effects of the oblique angle on heat transfer from a uniformly heated plate to the impinging jet have been experimentally studied. The wall pres-

sure coefficients, the centerline velocity, and the near wall turbulent intensity profiles have also been presented.

It is observed that the stagnation point progressively shifts toward the minor flow region as the oblique angle decreases. It is also found that the position of the maximum turbulent intensity coincides with that of the stagnation point. The mean velocity profiles in the wall jet region have similarities where the downstream distance along the plate surface is larger than the nozzle-to-plate distance. It is also noted that the local Nusselt numbers in the minor flow region are larger than those in the major flow region for the same distance from the geometric center. This is attributed to the higher levels in turbulent intensity caused by more active mixing of the jet flow in the minor flow region. A correlation of the maximum Nusselt number in terms of the Reynolds number, the nozzle-to-plate distance, and the oblique angle has been presented.

# References

Baughn, J. W. and Shimizu, S., 1989, "Heat Transfer Measurement From a Surface With Uniform Heat Flux and an Impinging Jet," *ASME J. Heat Transfer*, Vol. 111, pp. 1096 ~1098.

Baughn, J. W., Hechanova, T. E. and Yan, X., 1991, "An Experimental Study on Entrainment Effects on the Heat Transfer From a Flat Surface to a Heated Circular Impinging Jet," ASME J. Heat Transfer, Vol. 113, pp. 1023~1025.

Chia, C., Giralt, F. and Trass, O., 1977, "Mass Transfer in Axisymmetric Turbulent Impinging Jet," *Industrial and Engineering Chemistry Fundamentals*, Vol. 16, pp. 28~35.

Foss, J. F. and Kleis, S. J., 1976, "Mean Flow Characteristics for the Oblique Impingement of an Axisymmetric Jet," *AIAA Journal*, Vol. 14, pp. 705~706.

Foss, J. F., 1979, "Measurement in a Large -Angle Oblique Jet Impingement Flow," *AIAA Journal*, Vol. 17, pp. 801~802.

Goldstein, R. J. and Franchett, M. E., 1988, "Heat Transfer From a Flat Surface to an Oblique Impinging Jet," *ASME J. Heat Transfer*, Vol. 110, pp. 84~90.

Gardon, R. and Cobonpue, J., 1962, "Heat Transfer Between a Flat Plate and Jets of Air Impinging on It," *ASME International Development in Heat Transfer*, pp. 454~459 .

Gardon, R. and Akfirat, J. C., 1965, "The Role of Turbulence in Determining the Heat Transfer Characteristics of Impinging Jets," *Int. J. Heat Mass Transfer*, Vol. 8, pp. 1261~1272.

Gardon, R. and Akfirat, J. C., 1966, "Heat Transfer Characteristics of Impinging Two -Dimensional Air Jets," *ASME J. Heat Transfer*, Vol. pp. 101~108.

Hoogendoorn, C. J., 1977, "The Effect of Turbulence on Heat Transfer at Stagnation Point," *Int. J. Heat Mass Transfer*, Vol. 20, pp. 1333~1338.

Ichimiya, K., 1995, "Heat Transfer and Flow Characteristics of an Oblique Turbulent Impinging Jet Within Confined Walls," *Int. J. Heat Transfer* Vol. 117, pp. 316~322.

Jambunathan, K. E., Lai, Moss, M. A. and Button, B. L., 1992, "A Review of Heat Transfer Data for Single Circular Jet Impingement," *Int. J. Heat and Fluid Flow*, Vol. 13, pp. 106~115.

Kataoka, K., 1990, "Impingement Heat Transfer Augmentation due to Large Scale Eddies," *Proc. of 9th Int. Heat Transfer Conference*, Vol. 1, pp. 255~273 .

Kline, S. J. and McKlintock, F. A., 1953, "Describing Uncertaintiesin Single Sample Experiments," *Mech. Engng*, Vol. 5, pp. 3~8.

Lee, S. J., Lee, J. H. and Lee, D. H., 1994, "Heat Transfer Measurements Using Liquid Crystal with an Elliptic Jet Impinging upon the Flat Surface," *Int. J. Heat Mass Transfer*, Vol. 37, pp. 967~976 .

Lee, D. H., Greif, R. S., Lee, J. and Lee, J. H., 1995, "Heat Transfer from a Surface to a Fully Developed Axisymmetric Impinging Jet," *ASME J. Heat Transfer*, Vol. 117, pp. 772~776.

Martin, H., 1977, "Heat and Mass Transfer between Impinging Gas Jets and Solid Surfaces," *Advances in Heat Transfer, Academic Press, New York*, Vol. 13, pp. 1~60.

Poreh, M., Tsuei, Y. G. and Cermak, J. E.,

1967, "Investigation of a Turbulent Radial Wall Jet," *Trans. ASME, J. Appl. Mech.*, pp. 457 ~463.

Sparrow, E. M. and Lovell, B. J., 1980, "Heat Transfer Characteristics of an Obliquely Impinging Circular Jet," *ASME J. Heat Transfer*, Vol. 102, pp. 202~209.

Stevens, J. and Webb, B. W., 1991, "Local Heat Transfer Coefficients Under an Axisymmetric, Single Phase Liquid Jet," *ASME J. Heat Transfer*, Vol. 113, pp. 71~78.

Tani, I. and Komatsu, Y., 1964, "Impingement of a Round Jet on a Flat Surface," *Proc. 11th*

*Congr. Appl. Mech., Munich*, pp. 672~676.

Viskanta, R., 1993, "Heat Transfer to Impinging Isothermal Gas and Flame Jets," *Experimental Thermal and Fluid Science*, Vol. 6, pp. 111 ~134.

Verhoff, A., 1963, "The two-dimensional turbulent wall jet with and without an external stream," Rep. 626, Princeton Univ..

Yan, X., 1993, "A Preheated-Wall Transient Method Using Liquid Crystals for the Measurement of Heat Transfer on External Surfaces and in Ducts," Ph. D. Dissertation, University of California, Davis.